Knockout of the high-coupling cytochrome aa_3 oxidase reduces TCA cycle fluxes in *Bacillus subtilis*

Nicola Zamboni, Uwe Sauer *

Institute of Biotechnology, ETH Zürich, CH-8093 Zürich, Switzerland

Abstract

The metabolic impact of electron rerouting in the respiratory chain of *Bacillus subtilis* was quantitatively assessed during batch growth of quinol oxidase mutants by ^{13}C-tracer experiments. While disruption of the low-coupling cytochrome *bd* oxidase was without any apparent phenotype, deletion of the high-coupling cytochrome aa_3 oxidase caused a severe reduction of tricarboxylic acid cycle fluxes and increased overflow metabolism. Since the product-corrected biomass yields were identical in mutants and parent, the results show that efficient ATP generation is not overly important for exponential growth of *B. subtilis* in batch culture.
© 2003 Federation of European Microbiological Societies. Published by Elsevier B.V. All rights reserved.

Keywords: Bioenergetics; Respiration; Tricarboxylic acid cycle; Metabolic flux analysis; Metabolic flux ratio analysis; Metabolic engineering

1. Introduction

Cellular energetics play a central role in microbial physiology and the question whether speed or efficiency of energy generation dictates the choice of parallel pathways for ATP production is of fundamental importance [1–3]. Aerobically, the primary source of ATP is oxidative phosphorylation and bacteria have modular, branched respiratory systems that drive this process depending on physiological demands and environmental conditions. Understanding the physiological function of branches with different energetic efficiencies in bacterial respiratory chains is an ongoing research topic [4,5]. Depending on the coupling efficiency of their components, branched respiratory chains of most microbes can translocate between zero and four protons per electron [6].

A prominent example for branched respiratory chains is the Gram-positive *Bacillus subtilis*, which contains at least three different terminal oxidases for the transfer of electrons from reducing equivalents to molecular oxygen [5].

The cytochrome *c* branch appears to be of marginal relevance under laboratory conditions [5,7,8]. The primary branches are the quinol oxidases cytochrome *bd* (encoded by *cydABCD*) and aa_3 (encoded by *qoxABCD*) that translocate one or two protons per electron transferred to oxygen, respectively. During well-aerated exponential growth in minimal or rich medium batch cultures, the cytochrome aa_3 oxidase appears to be predominant in *B. subtilis* [5,9], while the high-affinity cytochrome *bd* oxidases is more relevant at low oxygen tensions [10] and in well-aerated but glucose-limited chemostat cultures [7]. Either quinol oxidase, but not the cytochrome *c* oxidase, is fully capable of supporting growth alone [5,7]. Since about four protons are necessary for oxidative phosphorylation of ATP [11–13], *B. subtilis* can generate between 0.5 and 1 ATP per NADH, which corresponds to a maximal P-to-O ratio of unity that was hypothesized before [14].

The importance of altered respiratory energy generation on batch growth physiology is assessed here by quantification of the intracellular carbon flux responses to knockout of either quinol oxidase in the riboflavin-producing *B. subtilis* strain RB50::pRF69 [3,7,15]. For this purpose, we used metabolic flux ratio (METAFoR) analysis [16] and metabolic net flux analysis [17,18] based on gas chromatography-mass spectrometry (GC-MS)-analyzed amino acids from ^{13}C-labeling experiments [19–22].

* Corresponding author. Tel.: +41 (1) 633 3672;
Fax: +41 (1) 633 1051.
E-mail address: sauer@biotech.biol.ethz.ch (U. Sauer).

2. Materials and methods

2.1. Bacterial strains and growth conditions

In this study we used the *B. subtilis* strain RB50::pRF69, which is characterized by a deregulated riboflavin biosynthesis and bears one additional copy of the constitutively expressed, recombinant *B. subtilis rib* operon pRF69 integrated in the chromosome [15]. The *cydBC* and *qoxAB* mutations were introduced by PBS1 phage transduction [7].

Frozen stocks were used to inoculate 5 ml Luria–Bertani broth [23], containing neomycin at a final concentration of 5 mg l^{-1} when required. After 8 h incubation, 250 μl of this culture was used to inoculate 50 ml M9 [23] minimal medium with 10 g l^{-1} glucose in 500-ml baffled shake flasks. At the end of the exponential growth phase, 250 μl was used, in turn, to inoculate 50 ml M9 medium with 5 g l^{-1} glucose for physiological characterization. All cultures were incubated at 37°C on a gyratory shaker at 250 rpm. For ^{13}C-labeling experiments, glucose was added either entirely as the 1-^{13}C-labeled isotope isomer (Cambridge Isotopes, Andover, MA, USA) or as a mixture of 20% (w/w) [U-^{13}C]glucose (Martek Biosciences, Columbia, MD, USA) and 80% (w/w) natural glucose.

2.2. Analytical techniques

Cell growth was monitored by measuring the optical density with a spectrophotometer at 600 nm (OD$_{600}$) or with a Klett colorimeter (Bel-Art, Pequannock, NJ, USA) using a green filter (520–580 nm). Glucose and acetate concentrations in the supernatant were determined enzymatically (Beckman Synchron CX5CE). Acetoin was measured by GC analysis using a Carbowax MD-10 column (Macherey-Nagel) and riboflavin concentrations with a spectrophotometer at 440 nm upon dilution in 0.2 M NaOH. Specific consumption and production rates were calculated as described previously [24], using an experimentally determined factor of 0.33 g cellular dry weight (CDW) per OD$_{600}$ unit, and yields were calculated from the specific rates.

2.3. METAFoR analysis by GC-MS

Culture aliquots were harvested by centrifugation, washed once with 1 ml 0.9% NaCl, and hydrolyzed in 1.5 ml 6 M HCl at 105°C for 24 h in sealed microtubes. The hydrolysate was dried in a vacuum centrifuge at room temperature and derivatized at 85°C for 1 h in 50 μl tetrahydrofuran and 50 μl *N*-(*tert*-butyldimethylsilyl)-*N*-methyl-trifluoroacetamide. Derivatized amino acids were analyzed on a series 8000 GC, combined with an MD 800 mass spectrometer (Fisons Instruments, Beverly, MA, USA) as described previously [19].

The GC-MS-derived amino acid mass distributions were corrected for naturally occurring isotopes and used to calculate METAFoRs according to the probabilistic equations described for *Escherichia coli* by Fischer and Sauer [19] with two modifications. First, the Entner–Doudoroff pathway was omitted because it is not present in *B. subtilis* [18]. Second, the anaplerotic reaction is catalyzed in *B. subtilis* by pyruvate carboxylase and not phosphoenolpyruvate (PEP) carboxylase as in *E. coli*. Hence, the contribution of anaplerosis to the oxaloacetate pool was estimated from the mass distribution of pyruvate.

2.4. Estimation of metabolic net fluxes

A biochemical reaction network was constructed based on the model of Dauner and Sauer [25] as shown in Fig. 1. From this network, we obtained a stoichiometric matrix containing 23 unknown fluxes and 21 metabolite balances, including balances for the substrates and products glucose, acetate, riboflavin, CO_2 and O_2, and the cofactors NADH and NADPH. Precursor requirements for biomass formation were taken from Dauner and Sauer [25]. This system of linear equations is under-determined and a solution space with an infinite number of different flux vectors that fulfill the constraints exists [17,26]. Hence, additional constraints are required to uniquely solve the system and estimate the in vivo fluxes. For this purpose, a set of linearly independent equations were obtained from the METAFoRs, similar to a previous approach [18]. Specifically, the following flux relationships were added as additional constraints to solve the system:

1. the fraction of serine derived through glycolysis:

$$a = \frac{2(v_6 - v_8 - v_9)}{2v_6 + v_7 + v_8}$$

2. the fraction of oxaloacetate (OAA) originating from pyruvate:

$$b = \frac{v_{19}}{v_{16} + v_{192}}$$

3. the fraction of PEP originating from OAA:

$$c = \frac{v_{18}}{v_{11} + v_{18}}$$

4. the upper and lower bounds for pyruvate originating from malate:

$$d \geq \frac{v_{17}}{v_{12} + v_{17}} \geq e$$

5. the upper bound of PEP originating through the pentose phosphate (PP) pathway:

$$f \geq \frac{v_7 + 3v_8 + 2v_9}{2v_6 + v_7 + v_8}$$

The sum of the weighted square residuals of the constraints from both metabolite balances and flux ratios was minimized using the MATLAB function *fmincon*. The re-
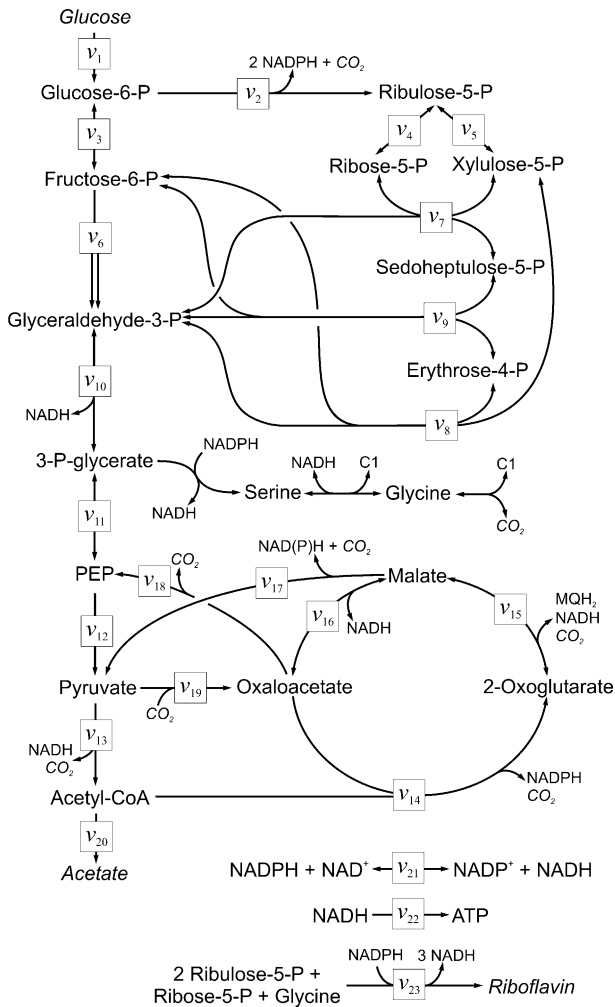
Fig. 1. Considered biochemical reaction network of *B. subtilis*. Arrows indicate the assumed reaction directionality or reversibility. Extracellular substrates and products are given in italics. MQH_2, menaquinol.

ent energetic efficiencies, we used two *B. subtilis* RB50::pRF69 mutants that were defective in the *cyd* and *qox* operons [7]. These mutants and their parent were grown in batch culture with glucose as the sole carbon source (Fig. 2). The *cyd* mutant grew essentially like its parent (Table 1), but a slight shift in byproduct formation with less acetate and more acetoin than the parent was discernible (Fig. 2). These physiological observations are consistent with the view that the *cyd* operon is primarily expressed at low oxygen tension, thus should not be active during the mid-exponential growth phase in well-aerated batch cultures [5,10]. In the *qox* mutant, in contrast, about 50% of the carbon substrate consumed during the exponential growth phase was secreted as acetate (Table 1 and Fig. 2), resulting in a significantly lower yield of biomass. This apparent yield reduction was quantitatively
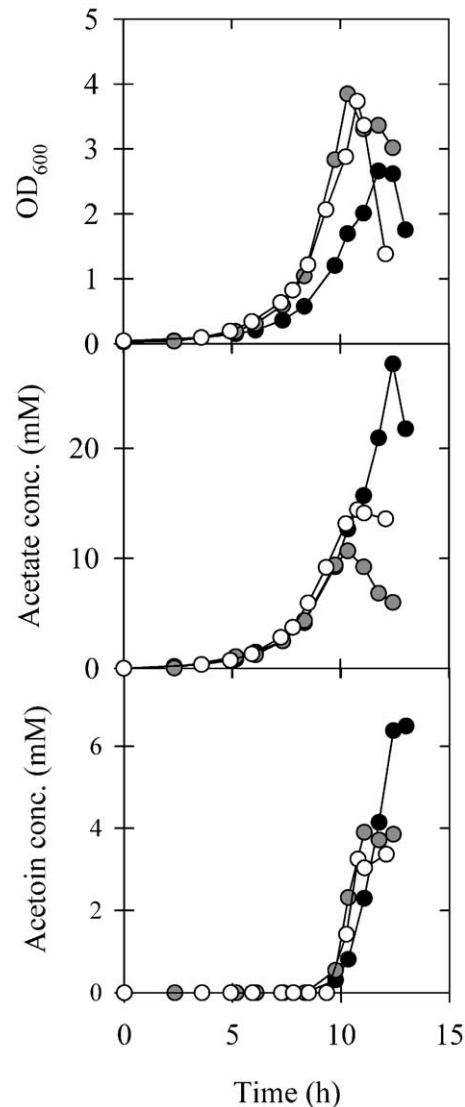
siduals were weighted by dividing through the experimental error. Thereby, only positive values were allowed for the irreversible reactions (Fig. 1). For flux ratios that were implemented as upper bounds, only error residuals from positive deviations from the experimental value were considered in the objective function, while for lower bounds, only negative deviations were considered. The computation was repeated at least five times with randomly chosen initial flux distributions to ensure identification of the global minimum. The Jacobian matrix of the output function was calculated to estimate the sensitivity of individual fluxes towards measurement errors, and confidence intervals were calculated for each flux.

3. Results and discussion

3.1. Physiological characterization

To investigate the metabolic impact of electron rerouting through branches of the respiratory chain with differ-

Fig. 2. Time profiles of OD_{600}, acetate, and acetoin concentrations during batch growth of *B. subtilis* RB50::pRF69 (white circles), RB50::pRF69 *cyd* (gray circles), and RB50::pRF69 *qox* (black circles) strains on glucose. The apparent lower growth rate of the *qox* mutant is not statistically significant (compare Table 1).

Table 1
Physiological parameters of *B. subtilis* respiratory mutants during exponential batch growth (between OD_{600} 0.5 and 1.5)

Strain	Maximum specific growth rate (1/h)	Specific uptake/consumption rates (mmol g CDW^{-1} h^{-1})		Biomass yield (g CDW g glucose^{-1})	
		Glucose	Acetate	Y	Y^{corr}
RB50::pRF69	0.44 ± 0.03	10.2 ± 0.8	5.8 ± 0.3	0.24 ± 0.02	0.33 ± 0.05
RB50::pRF69 *cyd*	0.48 ± 0.04	9.9 ± 0.1	4.6 ± 0.1	0.27 ± 0.02	0.35 ± 0.03
RB50::pRF69 *qox*	0.43 ± 0.03	11.8 ± 0.6	10.3 ± 0.2	0.20 ± 0.03	0.35 ± 0.04

Confidence intervals indicate the standard deviations from at least two experiments. The errors for the yields were calculated according to Gauss's law of error propagation. The biomass yield (Y^{corr}) was corrected for acetate formation.

accounted for by the increased byproduct formation and was not the consequence of a reduced respiratory coupling efficiency, since the product-corrected yields were 0.33–0.35 g CDW g glucose^{-1} for all three strains (Table 1).

3.2. Metabolic flux ratios in oxidase mutants

The physiological data suggested a major redistribution of carbon fluxes in the *qox* mutant. To identify this intracellular response, all three strains were grown in separate batch cultures with either 100% [1-^{13}C]glucose or a mixture of 20% [U-^{13}C]glucose and 80% unlabeled glucose. Biomass aliquots were collected at an OD_{600} of about 1.5 and 13 ratios of intracellular fluxes were determined with METAFoR analysis by GC-MS [19]. As expected the metabolic profiles of parent and *cyd* mutant were virtually identical (Fig. 3). While the METAFoR values of the *qox* mutant were similar in the PP pathway and in C1 metabolism, a major difference to the other strains was the fraction of OAA originating from pyruvate. This value quantifies the contribution of the anaplerotic reaction to OAA

synthesis, and the remaining percentage of OAA is derived through a full turn of the tricarboxylic acid (TCA) cycle. Thus, catabolic fluxes through the TCA cycle to OAA are very low in the *qox* mutant but are almost equally balanced with anaplerosis in the other two strains. This result was confirmed in a duplicate ^{13}C-labeling experiment with the *qox* mutant (data not shown). Along with the increased acetate production, this suggests that the fluxes in the TCA cycle are strongly reduced in the *qox* mutant.

3.3. Estimation of metabolic net fluxes

To gain more comprehensive insights, intracellular fluxes were estimated by quantitative balancing of the experimentally determined extracellular fluxes (Table 1), the detailed biomass composition of *B. subtilis* [25], and the METAFoR values of Fig. 3 as constraints. The available data were sufficient to resolve all reactions shown in Fig. 1 [27,28]. Consistent with the above results, parent and *cyd* mutant exhibited almost identical distributions of intracellular fluxes (Fig. 4). Almost all carbon fluxes were similar
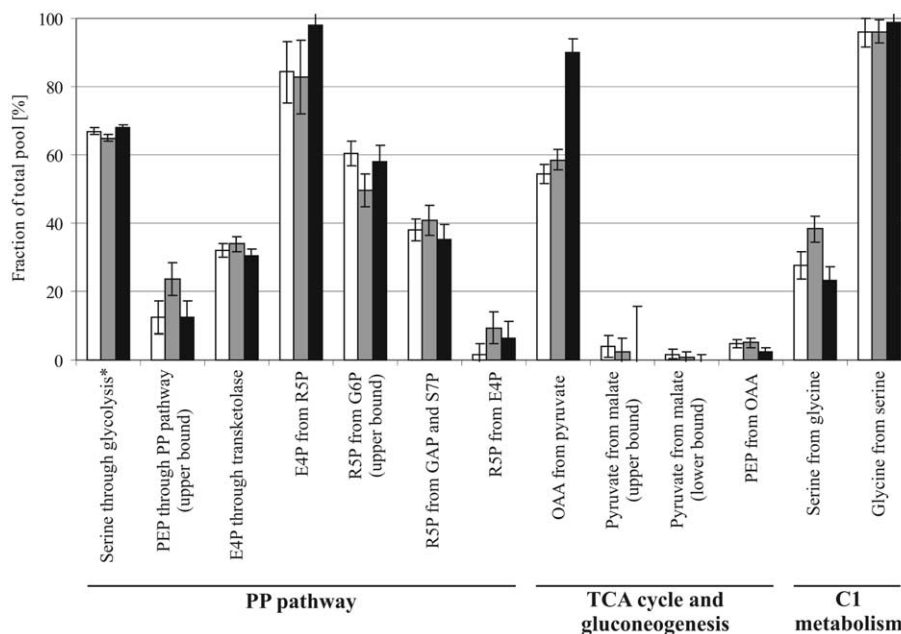

Fig. 3. Metabolic flux ratios of *B. subtilis* RB50::pRF69 (white bars), RB50::pRF69 *cyd* (gray bars), and RB50::pRF69 *qox* (black bars) during batch growth on glucose. E4P, erythrose-4-phosphate; GAP, glyceraldehyde-3-phosphate; G6P, glucose-6-phosphate; R5P, ribose-5-phosphate; S7P, sedoheptulose-7-phosphate.

in the *qox* mutant, with the TCA cycle flux and acetate overflow as the sole exceptions. As a consequence of this incomplete oxidation of glucose, significantly fewer reducing equivalents are generated and the calculated rate of respiration is reduced as indicated by the respiratory flux NADH to O_2. This reduced rate of respiration is probably catalyzed by the cytochrome *bd* oxidase that is encoded by the *cyd* operon [5], since a *cyd qox* mutant is not viable [5] or grows very poorly [7].

To elucidate the energetic impact of reduced coupling efficiency of respiration in the *qox* mutant, ATP production was assessed indirectly from the calculated net fluxes. For this purpose, we assumed exclusive operation of the low-coupling ($1 H^+/e^-$) cytochrome *bd* oxidase in the *qox* mutant and that four protons are used by the F_0F_1ATPase to produce 1 ATP [11,12]. Using these energetic parameters and the flux distribution shown in Fig. 4, which includes substrate-level phosphorylation and biosynthetic energy requirements, about 35% of the total energy generation was related to respiration. In total, an excess production of about 1.5 mol ATP per mol of consumed glucose was estimated for the *qox* mutant. For the parent strain, about 42% of the total ATP originates from respi-

ration and the ATP excess would be 0.9 and 3.2 mol mol^{-1} if exclusive operation of the cytochrome *bd* and aa_3 oxidases is assumed, respectively. This calculation does not account for non-growth-dependent maintenance requirements, which were previously estimated to be 5–8 mmol ATP per gram CDW and hour [7,29]. For the *qox* mutant this maintenance demand corresponds to 0.5–0.8 mol ATP per mol of consumed glucose during batch growth, hence about 30–50% of the excess ATP. Thus, we conclude that even exclusive operation of low-coupling oxidases such as cytochrome *bd* does not generate a situation with insufficient ATP supply during exponential growth on glucose.

More generally, the presented results indicate that the energetically more efficient cytochrome aa_3 oxidase is important during exponential growth in batch culture as was shown before [5,8], while the less efficient cytochrome *bd* is more relevant in glucose-limited chemostat cultures [7] and under low oxygen tensions [10]. Increased overflow to acetate in the *qox* mutant is probably not caused directly by low TCA cycle capacity, which is a frequently suggested hypothesis for acetate overflow in wild-type strains [30,31]. Instead it is more likely that the rate of NADH oxidation via the remaining oxidases is insufficient to oxidize all catabolically generated NADH at the maximum growth rate. Consequently, acetate overflow results from a kinetic limitation of the remaining terminal oxidases to compensate for the loss of cytochrome aa_3 in the *qox* mutant, as was suggested for wild-type *E. coli* [32,33].
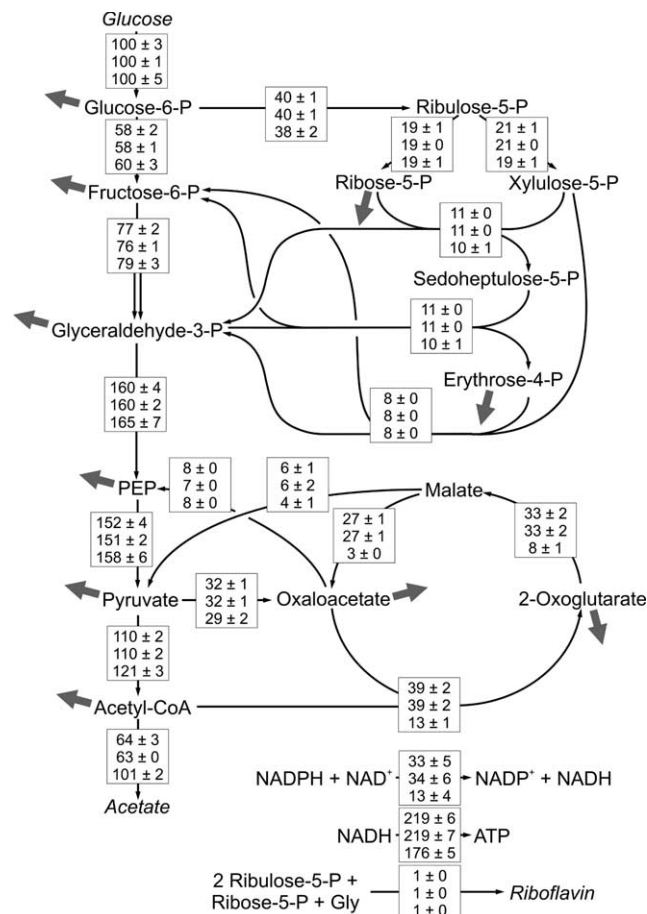
Fig. 4. Flux distributions of *B. subtilis* RB50::pRF69 (top values), RB50::pRF69 *cyd* (middle values), and RB50::pRF69 *qox* (bottom values) during exponential growth on glucose. Solid gray arrows indicate carbon fluxes to biosynthesis for which the values are not shown.

References

[1] Helling, R.B. (2002) Speed versus efficiency in microbial growth and the role of parallel pathways. J. Bacteriol. 184, 1041–1045.

[2] Pfeiffer, T., Schuster, S. and Bonhoeffer, S. (2001) Cooperation and competition in the evolution of ATP-producing pathways. Science 292, 504–507.

[3] Dauner, M., Storni, T. and Sauer, U. (2001) *Bacillus subtilis* metabolism and energetics in carbon-limited and excess-carbon chemostat culture. J. Bacteriol. 183, 7308–7317.

[4] Neijssel, O.M. and Teixeira de Mattos, M.J. (1994) The energetics of bacterial growth: a reassessment. Mol. Microbiol. 13, 172–182.

[5] Winstedt, L. and von Wachenfeldt, C. (2000) Terminal oxidases of *Bacillus subtilis* strain 168: one quinol oxidase, cytochrome aa_3 or cytochrome *bd*, is required for aerobic growth. J. Bacteriol. 182, 6557–6564.

[6] Trumpower, B.L. and Gennis, R.B. (1994) Energy transduction by cytochrome complexes in mitochondrial and bacterial respiration: The enzymology of coupling electron transfer reactions to transmembrane proton translocation. Annu. Rev. Biochem. 63, 675–716.

[7] Zamboni, N., Mouncey, N., Hohmann, H.P. and Sauer, U. (2003) Reducing maintenance metabolism by metabolic engineering of respiration improves riboflavin production by *Bacillus subtilis*. Metab. Eng. 5, 49–55.

[8] Lauraeus, M. and Wikström, M. (1993) The terminal quinol oxidases of *Bacillus subtilis* have different energy conservation properties. J. Biol. Chem. 268, 11470–11473.

[9] Santana, M., Kunst, F., Hullo, M.F., Rapoport, G., Danchin, A. and Glaser, P. (1992) Molecular cloning, sequencing, and physiological characterization of the *qox* operon from *Bacillus subtilis* encoding the aa_3-600 quinol oxidase. J. Biol. Chem. 267, 10225–10231.

[10] Winstedt, L., Yoshida, K., Fujita, Y. and von Wachenfeldt, C. (1998) Cytochrome *bd* biosynthesis in *Bacillus subtilis*: characterization of the *cydABCD* operon. J. Bacteriol. 180, 6571–6580.

[11] Saraste, M. (1999) Oxidative phosphorylation at the fin de siecle. Science 283, 1488–1493.

[12] Fillingame, R.H. (1997) Coupling H^+ transport and ATP synthesis in F_1F_0-ATP synthases: glimpses of interacting parts in a dynamic molecular machine. J. Exp. Biol. 200, 217–224.

[13] Pitard, B., Richard, P., Dunach, M. and Rigaud, J.L. (1996) ATP synthesis by the F_0F_1 ATP synthase from thermophilic *Bacillus* PS3 reconstituted into liposomes with bacteriorhodopsin. 2. Relationships between proton motive force and ATP synthesis. Eur. J. Biochem. 235, 779–788.

[14] Sauer, U. and Bailey, J.E. (1999) Estimation of P-to-O ratio in *Bacillus subtilis* and its influence on maximum riboflavin yield. Biotechnol. Bioeng. 64, 750–754.

[15] Perkins, J.B. et al. (1999) Genetic engineering of *Bacillus subtilis* for the commercial production of riboflavin. J. Ind. Microbiol. Biotechnol. 22, 8–18.

[16] Szyperski, T. (1995) Biosynthetically directed fractional ^{13}C-labeling of proteinogenic amino acids. An efficient analytical tool to investigate intermediary metabolism. Eur. J. Biochem. 232, 433–448.

[17] Szyperski, T. (1998) ^{13}C-NMR, MS and metabolic flux balancing in biotechnology research. Q. Rev. Biophys. 31, 41–106.

[18] Sauer, U., Hatzimanikatis, V., Bailey, J.E., Hochuli, M., Szyperski, T. and Wüthrich, K. (1997) Metabolic fluxes in riboflavin-producing *Bacillus subtilis*. Nat. Biotechnol. 15, 448–452.

[19] Fischer, E. and Sauer, U. (2003) Metabolic flux profiling of *Escherichia coli* mutants in central carbon metabolism using GC-MS. Eur. J. Biochem. 270, 880–891.

[20] Dauner, M. and Sauer, U. (2000) GC-MS analysis of amino acids rapidly provides rich information for isotopomer balancing. Biotechnol. Prog. 16, 642–649.

[21] Christensen, B. and Nielsen, J. (1999) Isotopomer analysis using GC-MS. Metab. Eng. 1, 282–290.

[22] Wittmann, C. and Heinzle, E. (1999) Mass spectrometry for metabolic flux analysis. Biotechnol. Bioeng. 62, 739–750.

[23] Harwood, C.R. and Cutting, S.M. (1990) in: Modern Microbiological Methods. John Wiley and Sons, Chichester.

[24] Sauer, U., Lasko, D.R., Fiaux, J., Hochuli, M., Glaser, R., Szyperski, T., Wüthrich, K. and Bailey, J.E. (1999) Metabolic flux ratio analysis of genetic and environmental modulations of *Escherichia coli* central carbon metabolism. J. Bacteriol. 181, 6679–6688.

[25] Dauner, M. and Sauer, U. (2001) Stoichiometric growth model for riboflavin-producing *Bacillus subtilis*. Biotechnol. Bioeng. 76, 132–143.

[26] Bonarius, H.P.J., Schmid, G. and Tramper, J. (1997) Flux analysis of underdetermined metabolic networks: The quest for the missing constraints. Trends Biotechnol. 15, 308–314.

[27] van der Heijden, R.T.J.M., Heijnen, J.J., Hellinga, C., Romein, B. and Luyben, K.C.A.M. (1994) Linear constraint relations in biochemical reaction systems: I. Classificatiopn of the calculability and the balanceability of conversion rates. Biotechnol. Bioeng. 43, 3–10.

[28] Klamt, S., Schuster, S. and Gilles, E.D. (2002) Calculability analysis in underdetermined metabolic networks illustrated by a model of the central metabolism in purple nonsulfur bacteria. Biotechnol. Bioeng. 77, 734–751.

[29] Sauer, U., Hatzimanikatis, V., Hohmann, H.-P., Manneberg, M., van Loon, A.P. and Bailey, J.E. (1996) Physiology and metabolic fluxes of wild-type and riboflavin-producing *Bacillus subtilis*. Appl. Environ. Microbiol. 62, 3687–3696.

[30] Fry, B., Zhu, T., Domach, M.M., Koepsel, R.R., Phalakornkule, C. and Ataai, M.M. (2000) Characterization of growth and acid formation in a *Bacillus subtilis* pyruvate kinase mutant. Appl. Environ. Microbiol. 66, 4045–4049.

[31] Majewski, R.A. and Domach, M.M. (1990) Simple constrained-optimization view of acetate overflow in *Escherichia coli*. Biotechnol. Bioeng. 35, 732–738.

[32] Han, K., Lim, H.C. and Hong, J. (1992) Acetic-acid formation in *Escherichia coli* fermentation. Biotechnol. Bioeng. 39, 663–671.

[33] el-Mansi, E.M. and Holms, W.H. (1989) Control of carbon flux to acetate excretion during growth of *Escherichia coli* in batch and continuous cultures. J. Gen. Microbiol. 135, 2875–2883.